Bond Performance of Near-Surface Mounted BFRP Bars to Concrete

Omar Aljidda
Ph.D. Candidate, Department of Civil and Water Engineering, Laval University, Quebec City, Quebec, Canada
omar.aljidda.1@ulaval.ca

Ahmed El Refai
Professor, Department of Civil and Water Engineering, Laval University, Quebec City, Quebec, Canada
ahmed.elrefai@gci.ulaval.ca

Wael Alnahhal
Associate Professor, Department of Civil and Architectural Engineering, Qatar University, Doha, Qatar
wael.alnahhal@qu.edu.qa

Abstract

This paper presents the test results of a study on the bond performance of near-surface mounted (NSM) basalt fiber reinforced polymer (BFRP) bars to concrete. Twelve C-shape concrete specimens were tested under direct pull-out loading configuration. Test parameters included the bar surface configuration (deformed and sand coated), the types of epoxy adhesive (NSM Gel and Sikadur-30), and the bonded length (6, 12, and 24 times its diameter). The influence of various parameters on the overall bond performance of NSM-BFRP bars is analyzed and discussed. The obtained results confirmed the impact of the investigated parameters on the bond behavior of the tested specimens. It was found that the bond strength and failure mode varied considerably with the bar surface configuration and bonded length. Higher bond strength was obtained when the NSM Gel epoxy with high strength properties. The results also revealed that both the deformed and sand coated bars showed almost similar bond strengths. Moreover, the pull-out loads increased with the increase of the bonded length of the NSM bars.

Keywords: Near-surface mounted; pull-out; Basalt; Strengthening

1 Introduction

The Near Surface Mounted (NSM) strengthening technique is one of the most effective techniques in strengthening existing reinforced concrete (RC) structural elements. The technique necessitates the use of strips or bars embedded in grooves that were made into the concrete cover and then filled with an appropriate filling material to ensure their bond to the concrete. Fiber-reinforced polymer (FRP) strips or bars are frequently used as NSM reinforcement because of their superior tensile strength and resistance to corrosion (Gómez, Torres & Barris, 2020); Maljaee, Ghiassi, & Lourenço, 2018); Novidis & Pantazopoulou, 2008). Previous research demonstrated that NSM-FRP bars may offer great anchorage capacity, resulting in high resistance against debonding, and therefore, a high ratio of the tensile strength of the FRP bars can be utilized (Kalupahana et al., 2013; De Lorenzis & Teng, 2007; De Lorenzis & Nanni, 2001).

The structural efficiency of the NSM strengthening techniques depends on several parameters, such as the groove dimension in which the NSM reinforcements are embedded, the bar surface configuration, the bonded length, and the most importantly, the bond performance between bar-epoxy interface and the concrete-epoxy interface. The stress transmission and the interaction

processes occur via both interfaces: the cylindrical contact surface between the NSM-FRP bar and the epoxy and the boundary between the concrete substrate and epoxy. Perfect bond at both interfaces lets stress transfer between the NSM-FRP bars, the epoxy, and the concrete and guarantees a good composite behavior. In either case, the force transfer occurs at an earlier stage of loading via the chemical adhesion between the NSM bar and the epoxy, whereas friction and mechanical interlocking take place at higher load levels (Novidis & Pantazopoulou, 2008).

The majority of the earlier investigations have focused on the evaluating the bond behavior of NSM-FRP bars made of carbon (CFRP) or glass (GFRP) (Sharaky et al., 2013; De Lorenzis & Teng, 2007; Cruz & Barros, 2002). De Lorenzis et al. (2002) conducted direct pull-out tests on 36 concrete specimens reinforced with NSM-CFRP and GFRP bars with various groove-filling materials, bonded lengths, and groove sizes. The authors stated that specimens with epoxy resin failed at the epoxy-concrete interface rather than the bar-epoxy interface, whereas those bonded with cement mortars failed by splitting the mortar cover due to its low tensile strength as compared to epoxy. In addition, specimens with cement mortars showed 70% lower capacity than their epoxy-filled counterparts. Moreover, for a given groove size, the load-bearing capacity increased, and the bond strength decreased as the bonded length increased in all specimens. Soliman et al. (2011) investigated the effect of the bonded length, the FRP bar size, and the adhesive type on the bond performance of NSM-GFRP and CFRP bars. The results showed that the specimens with epoxy had a higher bond strength of about 40-56% than the corresponding specimens with cement adhesive. It was also stated that by increasing the bonded length, the load capacity of the specimen improved, in contrast to increasing the size of the groove, where a significant impact on the failure load was not recorded. Regarding the failure mode, concrete tension failure was the dominant failure mode. Lee et al. (2013) evaluated the bond behavior of NSM-CFRP and GFRP bars. The results verified the effect of the bar surface configuration on the bond behavior such that the use of spirally wound and sand coated bars showed the best performance, whereas CFRP bars displayed a higher bond strength than those of GFRP. Likewise, using epoxy adhesives with greater bond strength increased the bond strength of the tested pull-out specimens.

Recently, the BFRP bars have become known as promising substitutes for GFRP bars. However, despite many studies, noticeable lack of studies on using the BFRP bars in the NSM strengthening technique can be observed. This paper reports the experimental investigation in which pull-out tests were performed while investigating test parameters. The outcomes of this research were considered to be important before recommending the use of the BFRP bar in NSM strengthening technique application.

2 Experimental Program

2.1 Specimen Details

Twelve C-shaped concrete specimens were constructed and tested in the laboratory using a modified pull-out test, as illustrated in Figure 1. A square groove was made into the concrete pull-out specimen along its center using a special diamond saw to accommodate the NSM bars. The dimensions of the grooves were determined based on the diameter of the bars used (10 mm) and the minimum dimensions suggested by ACI 440.2R-17 (2017) provisions of *1.5d_b*. Prior to placing the NSM-BFRP bar into the groove, epoxy was first added to the groove until it reached the desired bonded length. The specimen's surface was leveled, and any extra epoxy was removed. All BFRP bars were anchored using long steel tubes and filled with cement grout in accordance with ASTM D7205M-21(2021) requirements. The pull-out specimens were then cured for 14 days in the

laboratory, which was kept at a constant temperature of 22°C.
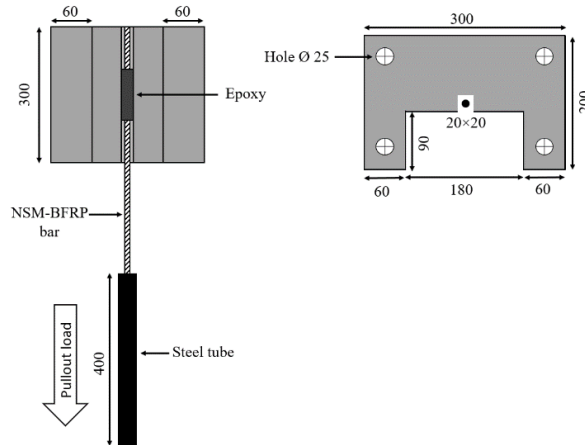
Fig. 1: Pull-out specimen (All dimensions are in *mm*)

2.2 Test Matrix

Various parameters were investigated in this study, including the bar surface texture (sand coated and deformed), the type of epoxy, and the bonded length ($6d_b$, $12d_b$, and $24d_b$), as summarized in Table 1. Each specimen is labeled in format A00-B. The first letter of the specimen's label, A, represents the bar surface configuration (SC for sand coated surface) and (D for deformed surface). The digits represent the bar's bonded length as a multiple of its diameter, while the letter B represents the type of epoxy (SD for Sikadure-30 epoxy) and (NG for NSM Gel). NSM-BFRP bars with a diameter of 10 mm embedded in a square groove of $2d_b$ are used in all specimens.

Table 1: Test Matrix

Specimen	Bar surface	Bonded length	Type of epoxy
D6-NG	Deformed	$6d_b$	NSM Gel
D6-SD	Deformed	$6d_b$	Sikadur-30
D12-NG	Deformed	$12d_b$	NSM Gel
D12-SD	Deformed	$12d_b$	Sikadur-30
D24-NG	Deformed	$24d_b$	NSM Gel
D24-SD	Deformed	$24d_b$	Sikadur-30
SC6-NG	Sand coated	$6d_b$	NSM Gel
SC6-SD	Sand coated	$6d_b$	Sikadur-30
SC12-NG	Sand coated	$12d_b$	NSM Gel
SC12-SD	Sand coated	$12d_b$	Sikadur-30
SD24-NG	Sand coated	$24d_b$	NSM Gel
SD24-SD	Sand coated	$24d_b$	Sikadur-30

2.3 Materials

All pull-out specimens were casted at the same time using ready-mix concrete with compressive strength at 28 days was 50 MPa. The mechanical properties of the sand coated and deformed BFRP bars were obtained from the manufacturer's datasheet, as summarized in Table 2. Two epoxies were used in the experimental study. The first type Sikadur-30 epoxy (SD), is a two-component epoxy, resins, and a special filler, designed for bonding structural reinforcement. The second type of epoxy NSM Gel (NG), is a high strength epoxy-based adhesive consisting of two parts resin and hardener. This epoxy is specially designed for NSM applications and may also be used for externally bonded

strengthening techniques. The epoxy properties are listed in Table 3.

Table 2: BFRP bars properties

Bar type	Bar surface	Tensile strength (MPa)	Ultimate strain%	Modulus of elasticity (GPa)
BFRP	Deformed	1200	2.31	52
BFRP	Sand coated	1278	2.22	57.5

Table 3: Epoxy properties

Epoxy type	Shear strength (MPa)	Modulus of elasticity (MPa)	Curing time
NSM Gel	27.2	1682	14 days
Sikadur-30	18	9600	7 days

2.4   Test setup

The pull-out tests were conducted using a Universal Testing Machine. A special steel frame setup, shown in Figure 2, was designed and fabricated to perform the tests. Each specimen was equipped with two LVDTs to measure the NSM bar's slippage at both loaded and free ends. The pull-out specimens were pulled with a displacement-controlled rate of 0.2 mm/min until failure. Outcomes from the LVDTs, the load cell, were collected using an automatic data acquisition system.
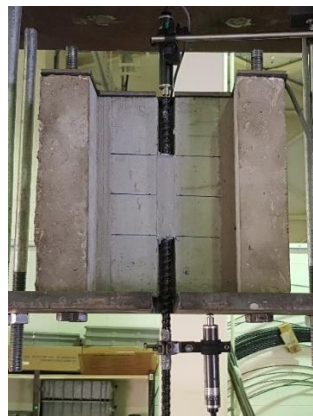
Fig. 2: Pull-out test setup

3 Experimental Results

The pull-out test results are listed in Table 4. The bond strength, τ_{max}, was calculated as per Equation (1) as follows:

$$\tau_{max} = \frac{P_{max}}{\pi d_b L_b}$$

(1)

Where P_{max} is the maximum pull-out force as obtained from the tests; d_b is the bar nominal diameter; L_b is the bonded length of the NSM bar.

Table 4: Pull-out test results

Specimens	P_{max} (kN)	τ_{max} (MPa)	$S_{max, le}$	$S_{max, fe}$	Failure mode
D6-NG	35.37	18.76	2.27	1.41	SEC
D6-SD	17.2	9.12	1.02	0.82	SEC
D12-NG	44.68	11.85	2.53	1.11	SEC
D12-SD	33.18	8.80	1.64	1.11	SEC
D24-NG	49.29	6.54	3.47	1.16	CS+ SEC

Specimens	P_{max} (kN)	τ_{max} (MPa)	$S_{max, le}$	$S_{max, fe}$	Failure mode
D24-SD	41.70	5.53	2.19	1.23	CS+ SEC
SC6-NG	33.42	17.73	2.24	1.08	P-SD
SC6-SD	31.66	16.80	2.01	0.82	P-SD
SC12-NG	44.26	11.74	4.09	1.64	P-SD
SC12-SD	33.47	8.88	1.77	0.76	P-SD
SC24-NG	49.86	6.61	3.31	1.40	CS+ P-SD
SC24-SD	49.14	6.52	3.31	1.12	CS+ P-SD

SEC= splitting of the epoxy cover; CS= concrete splitting; P-SD= NSM bar pull-out and surface delamination.

3.1 Failure Modes

- **Splitting of the epoxy cover**

This failure mode for all pull-out tested specimens with deformed bars surface with bonded lengths of $6d_b$ and $12d_b$, failure occurred by splitting of the epoxy cover companied by a varying degree of detachment of the concrete cover along the bar's bonded length were observed on most specimens, as shown in Figure 3(a).

- **NSM-bar pull-out and surface delamination**

This failure mode for all the specimens with sand coated bar surface texture with bonded lengths of $6d_b$ and $12d_b$. The bar's outer surface layer was entirely peeled off (delaminated) from the subsequent bar layers, as shown in Figure 3 (b).

- **Concrete splitting**

This failure mode characterized all pull-out tested specimens with a bonded length of $24d_b$. The crack started longitudinally at the loaded end and spread towards the free end along the center of the pull-out specimen, causing concrete splitting of the pull-out specimen, as shown in Figure 3 (c). It should be stated that this failure was brittle, with no earlier sign of cracking detected on the concrete surface.

(a)   (b)

(c)

Fig. 3: Mode of Failure: (A) D12-NG; (B) SC12-NG; (C) D24-NG

3.2 Bond Stress-Slip Relationship

Figure 4 presents representative average bond stress versus free and loaded ends slip relationships for NSM-BFRP specimens with a bonded length of $12d_b$ with different bar surface configurations. Each bond stress-slip curves demonstrated a linear ascending branch up to maximum bond stress. At the beginning of loading, the pull-out load increased linearly with the slow increase of the relative slip up to 50-60% of the maximum bond stress, and there have been no cracks in either the concrete or epoxy. After reaching the maximum bond stress, explosive sounds were heard, showing signs of cracking in the concrete surrounding the groove and the epoxy cover. Additional increase in the pull-out load resulted in additional cracks that spread longitudinally in the epoxy towards the bar's free end, and further slippage between the bar and the epoxy was observed. Once achieving the maximum stress, the bond stress-slip curves exhibited an abrupt descending branch that was described by a considerable decrease in the bond stress accompanied by a significant increment in the NSM-bar slippage. This sudden loss of bond described the loud explosive noise when the pull-out specimens achieved their maximum load. This was attributed to the epoxy splitting in the case of deformed NSM-BFRP specimens and bar surface delamination for the specimens with sand coated NSM-BFRP bars.
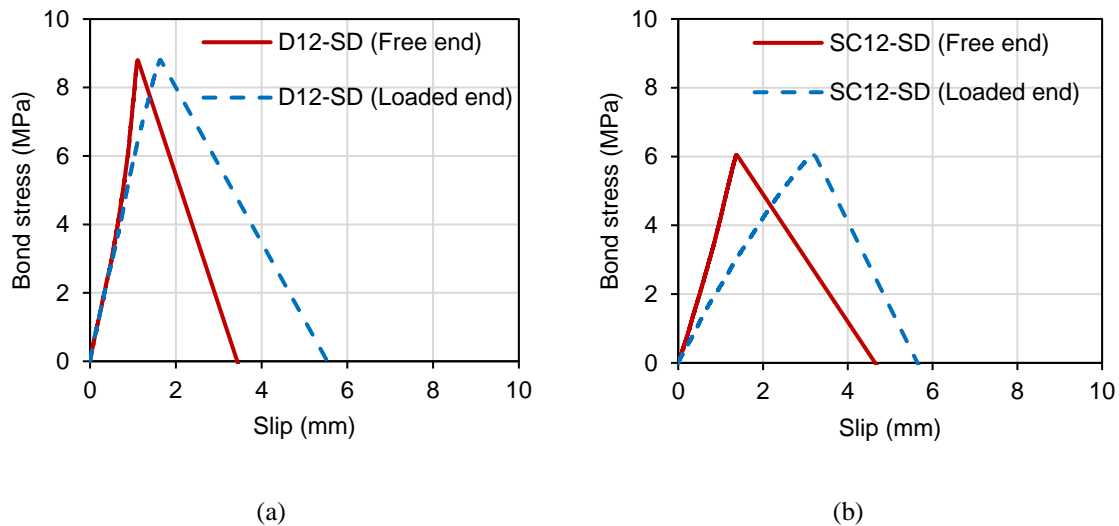

(a)   (b)

Fig. 4: Bond stress-slip curves: (A) D12-SD; (B) SC12-SD

3.3 Effect of Test Parameters

• Effect of The Type of Epoxy

Chemical adhesion is distinguished by a resistance to material separation. Therefore, the type of epoxy plays a significant role in ensuring a sufficient bond stress transfer from NSM bars to the concrete substrate. As plotted in Figure 5, the pull-out specimens with NG epoxy exhibited higher bond strength than the pull-out specimens with SD epoxy regardless of the bar surface configuration and bonded length due to high shear strength, as shown in Table 3. For example, the bond strength of specimens D12-NG and D12-SD were 11.9 and 8.9 MPa, respectively. A similar trend was observed for the specimens with different bonded lengths and the specimens with sand coated bar surface configuration, as illustrated in Figure 5.
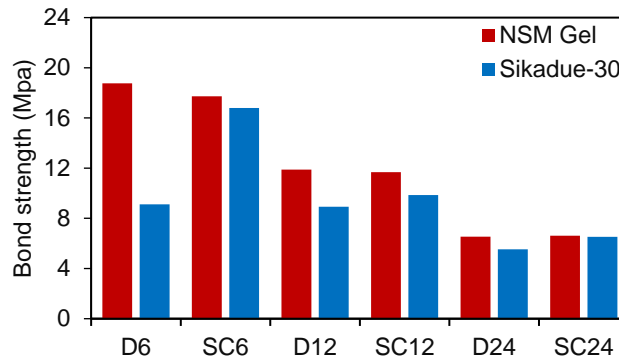
Fig. 5: Effect of the type of epoxy

- **Effect of the Bonded Length**

Relationships between the average bond strength and the bonded length are illustrated in Figure 6 for the specimens with different types of epoxy. In general, increasing the bonded length (L_b) leads to an increase in the maximum pull-out force (P_{max}). Contrarily, the average bond strength decreases due to the higher bonded area between the NSM bar and surrounding epoxy, as can be depicted from equation (1), and the non-uniform distribution of the bond stresses along the embedded portion of the bar, which increases with the increase of the bonded length, regardless of the type of the epoxy or bar surface texture. For example, the bond strengths of specimens with deformed BFRP bars decreased by 37% and 45% when their bonded lengths increased from $6d_b$ to $12d_b$ and $24d_b$, respectively. A similar trend was also observed by comparing the bond strength of the specimens with sand coated BFRP bars. The bond strengths decreased by 34% and 44% when their bonded length increased from $6d_b$ to $12d_b$ and $24d_b$, respectively.
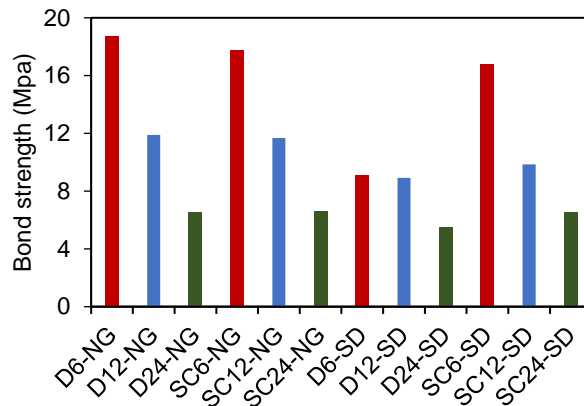

Fig. 6: Effect of the Bonded Length

- **Effect of the Bar Surface Configuration**

The bar surface configuration is critical to the bond behavior of NSM reinforcement because it directly affects the efficiency of the stress transfer from the NSM bar to the surrounding epoxy and concrete substrate through mechanical interlocking and frictional mechanisms (Wang & Cheng, 2021; Hassan & Rizkalla, 2004). As a result, several techniques, such as surface deformations or sand coating, or a combination of both, can be used to improve bond performance. The present experimental results showed that the bar surface configuration also governed the failure mode of the tested pull-out specimens. As shown in Table 4, all specimens with deformed BFRP bars failed due

to splitting their epoxy cover regardless of the epoxy type. The deformed surface configuration performed a significant role in improving the mechanical interlocking between the NSM-BFRP bar and the surrounding epoxy, which let the pull-out specimens develop their bond strengths. While the sand coated BFRP bars failed due to the delamination of the outer sand layer of the BFRP when the bar was pulled out. However, the epoxy surrounding the bar and the concrete remained undamaged along the bonded length indicated that the bond strength of the sand coated NSM-BFRP bar was developed mainly by friction and adhesion. However, the test results showed that the bar surface configuration had a minor impact on the bond strength of the pull-out tested specimens. This finding can be illustrated from the pull-out results shown in Figure 7.
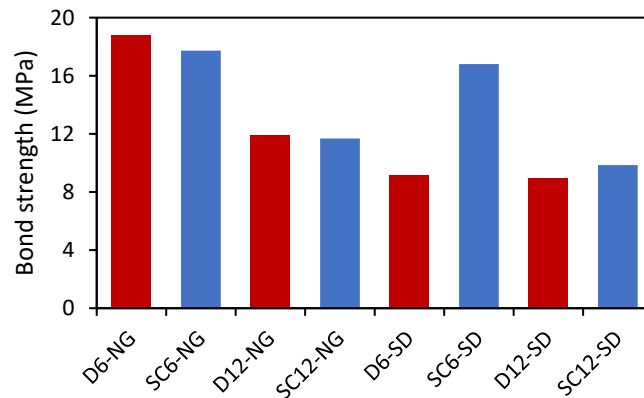

Fig. 7: Effect of the Bar Surface Configuration

4 Conclusion

This paper presented experimental investigations concerning the bond performance of BFRP bars when used for NSM application. From the experimental test results, the following conclusions are drawn:

1. The sand coated BFRP specimens with bond lengths of *6d$_b$* and *12d$_b$* failed due to NSM bar pull-out and surface delamination, while their deformed counterparts failed due to the splitting of the epoxy cover.

2. The concrete splitting was governor failure mode for the pull-out specimens with the bonded length of *24d$_b$*.

3. The epoxy's shear strength had a major impact on the bond behavior. The pull-out specimens with NSM Gel showed the best reliability producing the highest bond strength.

4. Increasing the bonded length caused a significant increase in the pull-out loads. However, the average bond strength decreased because of the non-uniform distribution of bond stress along the bonded length.

5. The sand coated and deformed NSM-BFRP bars exhibited almost similar bond strengths. The bar surface configuration had a slight impact on the bond strength of the tested specimens.

References

ACI 440.2R-17. (2017). *Guide for the Design and Construction of Externally Bonded FRP Systems for Strengthening Concrete Structures.*

ASTM D7205/D7205M-21. (2021). *Standard Test Method for Tensile Properties of Fiber Reinforced Polymer Matrix Composite Bars 1*. https://doi.org/10.1520/D7205_D7205M-21

Cruz, J. M. S. & Barros, J. A O. (2002). Bond Behavior of Carbon Laminate Strips into Concrete By Pull-out-Bending Tests. *"Bond in Concrete – from Research to Standards," 2002*, 8.

De Lorenzis, L. & Nanni, A. (2001). Characterization of FRP Rods as Near-Surface Mounted Reinforcement. *Journal of Composites for Construction*, *5*(2), 114–121. https://doi.org/10.1061/(asce)1090-0268(2001)5:2(114)

De Lorenzis, L., Rizzo, A. & La Tegola, A. (2002). A modified pull-out test for bond of near-surface mounted FRP rods in concrete. *Composites Part B: Engineering*, *33*(8), 589–603. https://doi.org/10.1016/S1359-8368(02)00052-5

De Lorenzis, L., & Teng, J. G. (2007). Near-surface mounted FRP reinforcement: An emerging technique for strengthening structures. *Composites Part B: Engineering*, *38*(2), 119–143. https://doi.org/10.1016/j.compositesb.2006.08.003

Gómez, J., Torres, L. & Barris, C. (2020). Characterization and simulation of the bond response of NSM FRP reinforcement in Concrete. *Materials*, *13*(7). https://doi.org/10.3390/MA13071770

Hassan, T. & Rizkalla, S. H. (2004). Bond Mechanism of Near Surface Mounted Fiber Reinforced Polymer Bars for Flexural Strengthening of Concrete Structures. *Repair and Strengthening of Concrete Structures*, *101*(6), 830–839. https://doi.org/10.1680/frasocs.16156.0003

Kalupahana, W. K. K. G., Ibell, T. J. & Darby, A. P. (2013). Bond characteristics of near surface mounted CFRP bars. *Construction and Building Materials*, *43*, 58–68. https://doi.org/10.1016/j.conbuildmat.2013.01.021

Lee, D., Cheng, L. & Yan-Gee Hui, J. (2013). Bond Characteristics of Various NSM FRP Reinforcements in Concrete. *Journal of Composites for Construction*, *17*(1), 117–129. https://doi.org/10.1061/(asce)cc.1943-5614.0000318

Maljaee, H., Ghiassi, B. & Lourenço, P. B. (2018). Bond behavior in NSM-strengthened masonry. *Engineering Structures*, *166*(April), 302–313. https://doi.org/10.1016/j.engstruct.2018.03.091

Novidis, D. G., & Pantazopoulou, S. J. (2008). Bond tests of short NSM-FRP and steel bar anchorages. *Journal of Composites for Construction*, *12*(3), 323–333. https://doi.org/10.1061/(ASCE)1090-0268(2008)12:3(323).

Sharaky, I. A. et al. (2013). Effect of different material and construction details on the bond behaviour of NSM FRP bars in concrete. *Construction and Building Materials*, *38*, 890–902. https://doi.org/10.1016/j.conbuildmat.2012.09.015

Soliman, S. M., El-Salakawy, E. & Benmokrane, B. (2011). Bond performance of near surface mounted FRP bars. *Journal of Composites for Construction*, *15*(1), 103–111. https://doi.org/1090-0268/2001/1-103-111/$25.00.

Wang, X. & Cheng, L. (2021). Bond characteristics and modeling of near-surface mounted CFRP in concrete. *Composite Structures*, *255*(August 2020). https://doi.org/10.1016/j.compstruct.2020.113011